Analysis of ASTER Emissivity Product Over an Arid Area in Southern New Mexico, USA

Maria Mira, Thomas J. Schmugge, *Fellow, IEEE*, Enric Valor, Vicente Caselles, and César Coll

***Abstract*—The accuracy of thermal infrared emissivities derived from Advanced Spaceborne Thermal Emission and Reflectance radiometer (ASTER) was assessed in an arid area in southern New Mexico, which includes the White Sands National Monument (WSNM) during 2006–2008. ASTER emissivities retrieved by the temperature and emissivity separation (TES) algorithm were directly compared with laboratory measurements of samples from WSNM. Good agreement was found for the high spectral contrast of gypsum and for the low spectral contrast of water bodies. Furthermore, the day/night consistency of ASTER emissivities was checked, and day/night emissivity differences lower than ± 0.013 were observed. However, unexpected emissivity values larger than unity were retrieved by ASTER/TES at 8–9 μm, mainly concentrated over lava flow surfaces. The thermal infrared radiance image data with 90-m spatial resolution was resized to 180 m for the analysis in this paper to avoid misregistration problems due to terrain topography. Emissivity temporal variations were analyzed and attributed, in some cases, to the soil moisture variations. This was particularly noted after periods of high precipitation which occurred in August 2006. The results presented here show the high emissivity accuracy achievable with ASTER data in ideal atmospheric conditions and discuss some problems which should be considered in the future, as the retrieval of overestimated emissivity values.**

***Index Terms*—Emission, infrared measurements, moisture, remote sensing, soil.**

I. Introduction

EMISSIVITY is the physical property which defines the capability of a body to radiate and absorb energy from the environment. It is defined as the ratio between the real emission of an object and the emission of a black body at the object thermodynamic (or kinetic) temperature [1]. The emissivity of natural surfaces is a magnitude required for the determination of accurate land surface temperature (LST) from thermal infrared (TIR) radiance measurements. If emissivity is not well determined, it can cause a significant error in obtaining LST, since an emissivity variation of 0.06 causes an error up to 2.2 K in the LST determination (at 11 μm for an LST of about 300 K [2]).

LST and emissivity products are generated by a number of spaceborne sensors such as the Advanced Spaceborne Thermal Emission and Reflectance radiometer (ASTER) [3], the Moderate resolution Imaging Spectroradiometer (MODIS) [4], and the Atmospheric Infrared Sounder (AIRS) [5] at varying spatial, spectral, and temporal resolutions. Both parameters are essential for a wide range of studies, undertaken at a variety of spatial scales, such as environmental monitoring, geological mapping, and hazard prediction. Emissivity spectra also provide important information on the mineral composition of land surfaces [6]–[9].

The North American ASTER Land Surface Emissivity Database (NAALSED) [10] provides a mean, seasonal, gridded LST, and emissivity database at 90-m spatial resolution based on the ASTER emissivity product, and it has been validated against geologic samples from large sand dune fields in the west and midwest U.S. [11]. Results indicate that the mean emissivity difference between NAALSED and the validation sites is typically less than ± 0.016.

The objective of this study is to contribute to the long-term accuracy assessment of the TIR emissivities derived from ASTER data, using the data taken during the period 2006–2008 for an arid area located at southern New Mexico (U.S.) for several different reference test sites.

II. Study Area

The study area is in the arid Tularosa Basin in southern New Mexico (U.S.). The different study sites, located in Fig. 1 and detailed in Table I, are White Sands dune field, Lake Lucero, Alkali Flat, and the lava flow of the "Valley of Fires." The area provides an excellent test case for thermal remote sensing since it encompasses a broad range of emissivities from the high spectral contrast of gypsum at the White Sands to the gray body behavior of water or the high emissivity values over the lava flow.

The White Sands dune field (Fig. 1) is located within the Tertiary Rio Grande Rift of Colorado, New Mexico, and Texas. It is of geological recent formation (approximately 7000 years old [12]). The rift contains numerous basins, including the Tularosa Basin, which is a downfaulted arid to semiarid area covering about 17 000 km^2 of south-central New Mexico. The gypsum dunes of White Sands lie in the Tularosa Basin, between the San Andres Mountains to the west and the Sacramento Mountains

Manuscript received February 5, 2010; revised May 18, 2010; accepted July 8, 2010. Date of publication September 23, 2010; date of current version March 25, 2011. This work was supported in part by the Generalitat Valenciana under Grant PROMETEO/2009/086 and in part by the European Space Agency under SMOS Cat-1 project AO-4748. The work of M. Maria was supported by the Spanish Ministry of Science and Innovation under Projects CGL2007-64666/CLI, CGL2007-29819-E/CLI, and CGL2009-07983, which are cofinanced by FEDER funds. The work of Dr. T. J. Schmugge was supported by the Gerald Thomas Endownment at New Mexico State University.

M. Mira, E. Valor, V. Caselles, and C. Coll are with the Department of Earth Physics and Thermodynamics, Faculty of Physics, University of Valencia, 46100 Burjassot, Spain (e-mail: Maria.Mira@uv.es).

T. J. Schmugge is with the Physical Science Laboratory, New Mexico State University, Las Cruces, NM 88003 USA.

Color versions of one or more of the figures in this paper are available online at http://ieeexplore.ieee.org.

Digital Object Identifier 10.1109/TGRS.2010.2061858

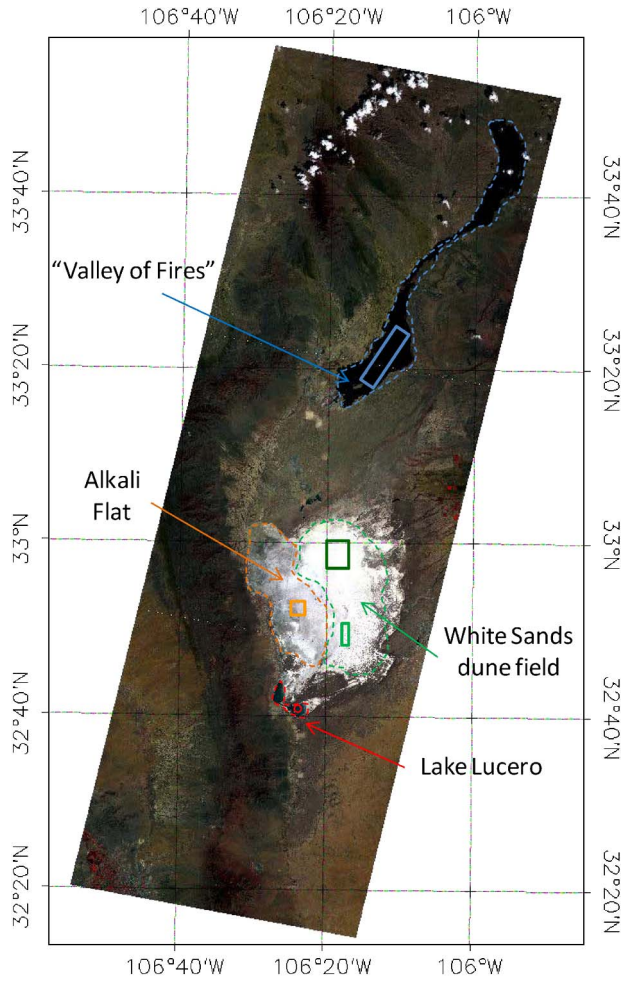

Fig. 1. RGB composite of ASTER bands 3 (0.556 μm), 2 (0.661 μm), and 1 (0.807 μm), degraded from the original 15 to 180-m spatial resolution, showing the White Sands desert area and environs on April 27, 2007. The target areas selected for the study are indicated with marks: (light green rectangle) Dune-1, (dark green rectangle) Dune-2, (red point) Lake Lucero, (orange square) Alkali Flat, (blue rectangle) lava flow.

to the east. White Sands is the world's largest gypsum dune field, encompassing 400 km^2 of white sand dunes, composed of hydrous calcium sulphate (gypsum). It consists of Aeolian gypsum deposits across barchan-transverse, parabolic, and barchan dunes derived through deflation from the evaporate beds of Lake Otero and the younger playa lakes [13]. The dunes were classified and mapped by [14]. Today, the gypsum sand is derived from the edge of the deflation basin, next to the dune field, rather than the Alkali Flat and playa lakes, where gypsum crystals are forming. The current dune field is considered a wet Aeolian system because the perched shallow water table controls the behavior of the accumulation surface over time. There is little or no vegetation present in the White Sands dune field, which is adjacent to the surrounding dark adobe soil of the Tularosa basin.

At least 20 playa lakes fill basins in the sediments of Lake Otero, the ancient lake. The largest of the playas, Lake Lucero (see Fig. 1), lies upwind of the dune field and is the major source of the gypsum sand. It consists of three subbasins in the shape of an L. The surface of the lake is a crust of white powdery gypsum with patches of halite. Below this crust, there are 10-cm-thick beds of clay, gypsiferous clay, and coarse gypsum crystals. Several additional playa lakes with features similar to Lake Lucero are found to the north.

Between the dunes and the playa lakes lies the Alkali Flat (see Fig. 1), an extensive, desolate, and largely unvegetated expanse. Patches of blowing gypsum sand lie within salt flats and areas of scattered bushes (i.e., Mesquite and Salt Bush). The soils and vegetation are best developed on the eastern side of the Alkali Flat, and salt pans are concentrated to the west near the playa lakes.

North of White Sands is the "Valley of Fires" (see Fig. 1), a lava flow originated from volcanic vents 1000 years ago in central New Mexico. It is approximately 4.8 km wide, 50 m thick, and over 71 km long and is the youngest and best preserved lava flow on the mainland U.S. Spanish explorers called this extensive lava flow "malpaís" or badlands. The large expanse of black, twisted lava deposits set among barren land with sparse vegetation (Fig. 2) is extremely rough and broken and thus provides a good high-emissivity gray body.

Regarding the climatic conditions of the area, the Tularosa basin is a high desert area, averaging 1200 m in elevation, with hot summers (averaging 35 °C) and relatively mild winters, but nighttime temperatures often go below freezing. Precipitation averages about 20 cm per year, with most falling during summer monsoon season. Wind is the dominant climatic factor, especially from February to May, the time of the greatest dune movement. The dominant wind direction in White Sands is from southwest to northeast. During the beginning of year 2006, the climatic conditions on White Sands were very dry. There was a heavy rainfall in August 2006, followed by significant precipitation events also during September and October of that year. As a result, for the year 2006, White Sands had 45 cm of rain, more than twice the usual 20 cm, and the park was closed for almost a year due to flooding (David Bustos, personal communication). Fig. 3 shows the monthly precipitation records for White Sands from September 2005 to December 2006.

III. Emissivity Retrieval From ASTER

ASTER is a high spatial resolution multispectral imager on the Terra spacecraft—the first platform of the National Aeronautics and Space Administration's Earth Observing System—launched in December 1999. ASTER consists of three separate subsystems: the visible and near infrared (VNIR), the short-wave infrared (SWIR), and the thermal infrared (TIR) [3]. The ASTER/TIR subsystem has five spectral bands (bands 10–14 with effective wavelength 8.3, 8.6, 9.1, 10.7, and 11.3 μm, respectively) with a 90-m spatial resolution, a 60-km imaging swath, and a revisit time of 16 days. It has a maximum pointing angle of $\pm 8.6^\circ$. The radiometric accuracy is ± 1 K, and the radiometric precision is ≤ 0.3 K, both at 300 K [15]. The multispectral TIR capability is an exclusive feature of ASTER, which allows the retrieval of LST and emissivity spectra at high spatial resolution.

We used current ASTER on-demand L2 Surface Emissivity (AST_05) provided on scene-by-scene basis using the temperature and emissivity separation (TES) algorithm [16]. TES calculates a normalized temperature and an emissivity spectrum

TABLE I
LOCATION AND LAND COVER TYPE OF THE TARGET AREAS SELECTED FOR THE STUDY, INCLUDING NUMBER OF PIXELS AT 180-m SPATIAL RESOLUTION

Sites	Location center	Land cover type	Number of selected pixels at 180-m spatial resolution
Dune-1	32.8101° N 106.2964° W	Transverse gypsum dune	102
Dune-2	32.9924° N 106.3067° W	Barchan gypsum dune	432
Lake Lucero (flooded)	32.6816° N 106.3978° W	Water	62
Lake Lucero (not flooded)		Powdery gypsum with patches of halite	
Alkali Flat	32.9181° N 106.4021° W	Blowing gypsum sand within salt flats	290
Lava Flow	33.3148° N 106.2411° W	Basalt and sparse vegetation	411

Fig. 2. Photograph showing part of the "Valley of Fires" north of White Sands, New Mexico.

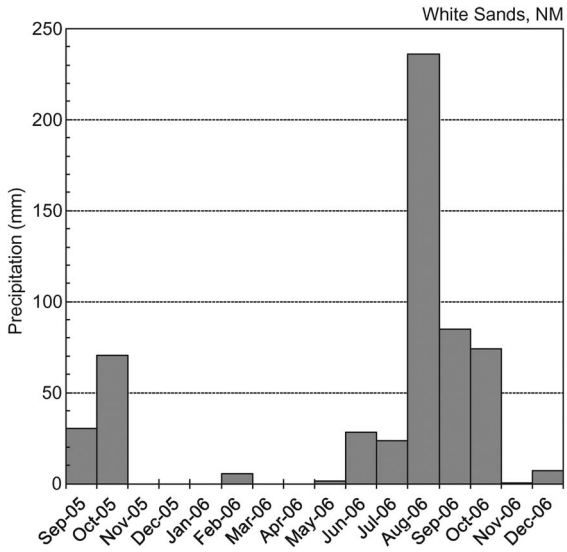

Fig. 3. Monthly precipitation data of White Sands, New Mexico for 2005–2006.

by means of the normalized emissivity method (NEM) [17]. TES can recover temperatures within ± 1.5 K and emissivities within ± 0.015 for a wide range of surfaces [16].

In this paper, 15 observations were used for the analysis of the ASTER emissivity product over our test area in southern New Mexico for the years 2006–2008. Each original scene is 830 $\times$ 700 pixels at 90-m spatial resolution. The data set consists of 11 daytime and 4 nighttime scenes and includes 3 day/night pairs close in time. The day and night time images were acquired at about 10:50 and 22:10 of the previous day (local time), respectively. The nighttime images were acquired on April 7, October 16, November 17, 2006, and April 26, 2007. The daytime images were acquired on April 8, November 18, December 4 and 29, 2006, April 4 and 27, 2007, January 1, February 2 and 18, March 5 and 12, 2008. All scenes are AST_05 (surface emissivity for TIR), while only 2006–2007 scenes are AST_07 (surface reflectance for VNIR and SWIR) and include White Sands dune field or the lava flow under clear sky conditions. AST_07 product was used to study the normalized difference vegetation index (NDVI) to detect the presence of water in Lake Lucero.

From the analysis of our data, overestimated (i.e., > 1.0) emissivity values were unexpectedly retrieved by ASTER/TES. Quantitatively, emissivities up to 1.018 were observed, with the highest emissivity values observed for band 11 (8.6 μm) and band 12 (9.1 μm), i.e., emissivities up to 1.004, 1.014, 1.018, 1.001, and 1.001 for ASTER bands 10 to 14, respectively. It is also worth noting that almost no scene acquired during 2008 contains emissivity values higher than 1.0, while every scene from 2006 to 2007 have values greater than 1.0.

Considering TIR emissivity of water (see Table II) and an ASTER accuracy of about ± 0.016 [11], emissivity values higher than 1.0 could be possible for ASTER band 10 (8.3 μm), band 13 (10.7 μm), and band 14 (11.3 μm) in the case of water bodies. However, emissivities higher than 1.002 or 1.003 observed by ASTER band 11 (8.6 μm) or band 12 (9.1 μm), respectively, are not justified even for water surfaces. Moreover, recall that TES usually underestimates emissivity of gray body scenes such as water [18]. Hence, the hypothesis of considering the unexpected overestimated emissivity retrievals due to high emissivity of water together with ASTER accuracy is not feasible.

The greatest number of pixels with unexpected emissivities higher than 1.0 are retrieved by ASTER band 10 (8.3 μm) and band 13 (10.7 μm) mainly over the "Valley of Fires," north of White Sands (see Fig. 4). Considering that the lava flow is a site with sparse vegetation, a first approximation for

TABLE II
LABORATORY SPECTRUM OF WATER, GYPSUM, AND BASALT, ACCORDING TO THE ASTER SPECTRAL LIBRARY [23] OR MEASUREMENTS FROM [29]

ASTER band	Gypsum	Water	Basalt
10 (8.3 μm)	0.935	0.983	0.960
11 (8.6 μm)	0.728	0.984	0.945
12 (9.1 μm)	0.869	0.985	0.911
13 (10.7 μm)	0.973	0.991	0.945
14 (11.3 μm)	0.977	0.990	0.949

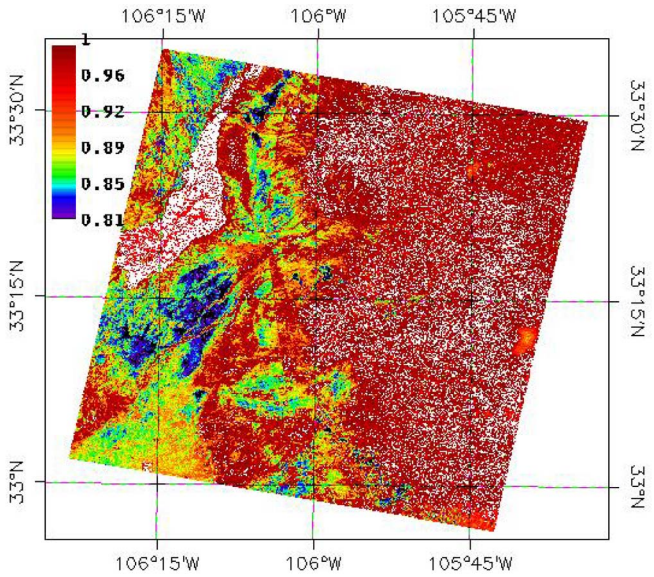

Fig. 4. ASTER emissivity scene at 180-m spatial resolution for band 10 (8.3 μm) showing southern part of the "Valley of Fires" and environs on April 4, 2007 (10:50 A.M., local time). Unexpected emissivities equal or higher than 1.0 were masked in white.

effective emissivity from such heterogeneous area can be estimated, not accounting for the cavity effect, using the following relationship [19]:

$$\varepsilon_i = \varepsilon_{\text{vegetation}_i} f + \varepsilon_{\text{basalt}_i}(1-f) \tag{1}$$

where subscript i refers to the spectral channel, and f is the fractional vegetation cover. Considering the vegetation as a gray body with emissivity 0.985, the basalt spectrum (see Table II), and an f value of about 0.5, emissivities could be up to 0.97. Then, even considering an ASTER accuracy of about ± 0.016, emissivity values higher than 1.0 retrieved over the lava flow cannot be justified in any case.

In our opinion, the problem of retrieving emissivities greater than unity is clearly an artifact of the processing algorithm. As shown by ASTER data for 2008, the changes introduced in the algorithm (e.g., iterative correction for downwelling irradiance and the threshold test for spectral contrast have been removed [20]) cleared up these discrepancies.

IV. RESULTS AND DISCUSSION

A. Day and Night Emissivities

The satellite viewing angle difference between day and night time ASTER observations can be up to $\pm 17.1^\circ$ since ASTER's cross-track pointing angle is $\pm 8.55^\circ$. In particular, it differs less than 8.6° for our pairs of day/night scenes. According to experimental studies [21]–[25], the observation angle effect on TIR emissivities may be significant at observation angles higher than 40°. Hence, we consider that the observation angle effects will be minimal on TIR emissivities when comparing day/night pairs of ASTER scenes.

However, it is known that ASTER has a geolocation problem for high-altitude sites since it determines the location assuming it to be at sea level. Hence, if ASTER is pointing off nadir, there is a location error proportional to the tangent of this angle and the altitude of the target. In our case, the study areas are at an altitude of about 1300 m, while the surrounding mountains are up to 2740 m in height. Considering the viewing angle (i.e., $\pm 8.55^\circ$), it leads to a geolocation error from 200 to 400 m (i.e., 3 to 5 ASTER/TIR pixels). Therefore, ASTER data were resampled to 180-m spatial resolution to avoid terrain effects. Nevertheless, for some targets (i.e., high-altitude locations) or situations (i.e., a day/night pair with a large viewing angle difference), it cannot be enough, leading to emissivity differences due to the geolocation error.

Fig. 5 shows an example of ASTER day and night emissivities for the 8.6-μm channel (band 11) and the 180-m spatial resolution for the area which overlaps the Alkali Flat and the gypsum dunes. As shown by the histograms, the day/night agreement is quite good. When studying the difference of images from day and night emissivity data, the images were georegistered manually to minimize the larger emissivity differences observed at the boundaries between the different cover types due to the geolocation problem. Note that the maximum occurs at a day/night difference of about -0.006, which is not a significant difference compared to the emissivity accuracy obtained by NAALSED validation results (± 0.016) [11].

Table III shows the ASTER emissivity difference observed between daytime and nighttime acquisitions. In addition, emissivities from gypsum and water targets were compared with those obtained from laboratory spectra available at the ASTER Spectral Library [26] and collected in Table II. Because scanning direction is opposite at day (i.e., descending) and night time (i.e., ascending), there are no day/night pairs coincident over the lava flow. With regard to the ASTER emissivities from the gypsum target (i.e., Dune-1 and Dune-2 sites), as specified in Table III, they are retrieved equally well by ASTER/TES both at day and night time. Their absolute emissivity difference is always less than 0.013, except for band 11 (8.6 μm) of the day/night pair from November 2006, for which it is 0.05. Although the low difference values, note that nighttime emissivities are higher than daytime emissivities (except for band 11 on April 26 and 27, 2007, Dune-2). This could be due to soil moisture effect on TIR emissivities, since dew could be present at night over the surface given the low nighttime temperatures. In addition, as specified in Table III, the high emissivity contrast of gypsum spectrum is observed quite well. When comparing ASTER emissivities from daytime acquisitions with gypsum spectrum from the ASTER Spectral Library, the results are encouraging, except for band 10 (8.3 μm) for which differences $\varepsilon_{\text{lab}} - \varepsilon_{\text{ASTd}}$ up to $+0.03$ are obtained. The same result was observed by [27], by comparing laboratory spectrum for

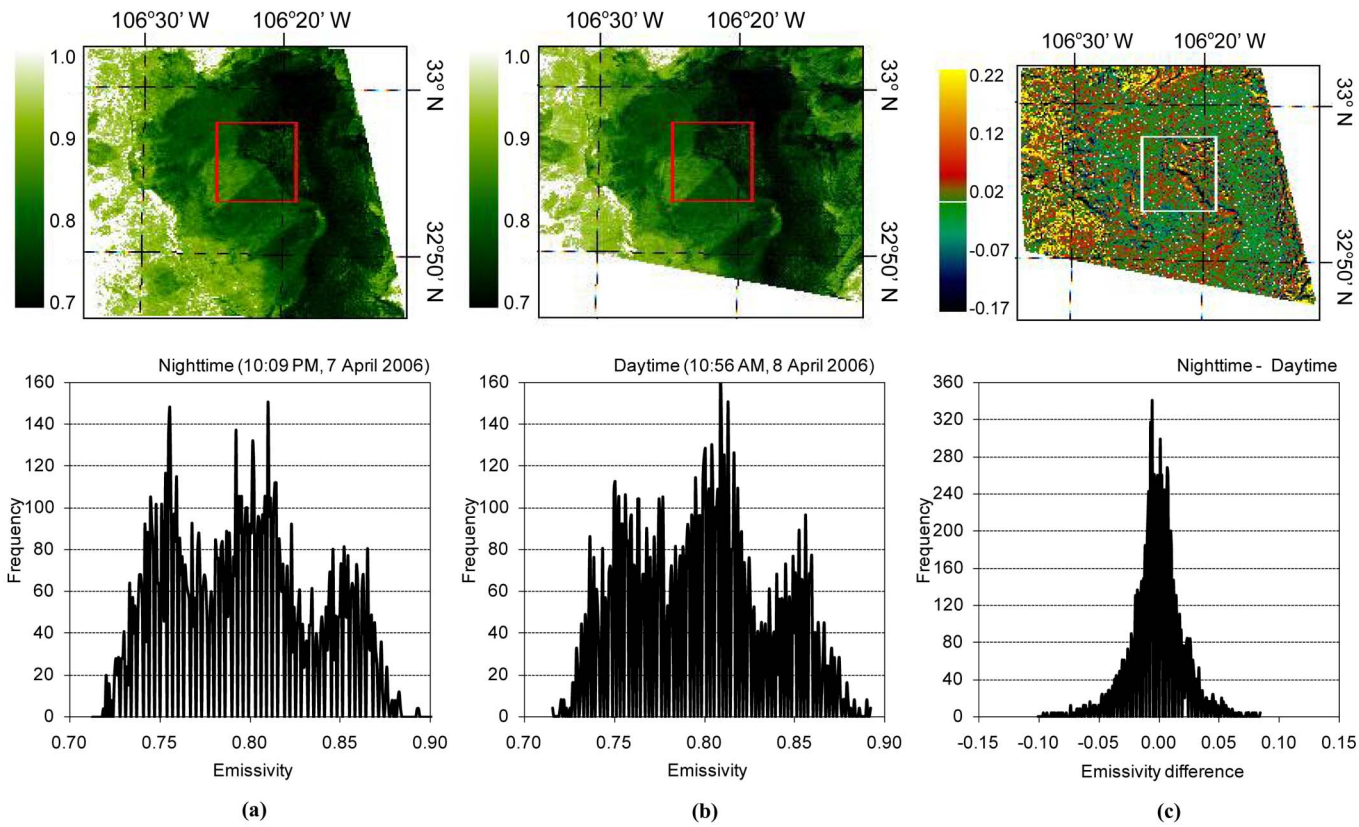

Fig. 5. Subset of an ASTER scene over a coincident target (i.e., part of the Alkali Flat and the White Sands dune field) and the histogram of pixels included within the red or white square, showing ASTER band 11 (8.6 μm) emissivity distribution at 180-m spatial resolution of (a) a night acquisition on April 7, 2006 (10:09 P.M., local time), (b) a day acquisition on April 8, 2006 (10:56 A.M., local time), and (c) the corresponding day/night difference $(\Delta\varepsilon = \varepsilon_{\mathrm{ASTn}} - \varepsilon_{\mathrm{ASTd}})$. The nighttime data were georegistered manually to the daytime data to minimize the terrain effects.

gypsum and ASTER emissivities acquired on 2000 and 2001 over gypsum dunes of White Sands. On the contrary, nighttime ASTER emissivities also disagree up to -0.05 for emissivities from band 11 (8.6 μm). As mentioned above, this last difference could be due to soil moisture effects, which increases TIR emissivities [2]. However, the low emissivities from band 10 retrieved in comparison to laboratory spectrum are still not explained.

For the Alkali Flat target, the ASTER day/night agreement is quite good, except for band 11 (8.6 μm) in which daytime emissivities are up to 0.04 higher than nighttime emissivities (see Table III). Until now, no sample from the Alkali Flat has been collected for laboratory measurements, hence direct comparisons with laboratory spectrum are not possible. However, its spectral shape is similar to that for gypsum sand but with a lower spectral contrast.

Analyzing the ASTER VNIR data (Fig. 1) and considering the precipitation records (Fig. 3) and the NDVI values for Lake Lucero (Fig. 6), it was observed that the lake was flooded with water in all scenes except for that from April 2006. NDVI values were computed by using surface reflectance corrected for atmospheric effects from visible and near infrared data at 0.661 μm (r_2) and at 0.807 μm $(r_{3\mathrm{N}})$ [28] of the AST_07 standard product as follows:

$$NDVI = \frac{r_{3N} - r_2}{r_{3N} + r_2}. \tag{2}$$

Negative NDVI values over Lake Lucero were associated with water bodies, while on April 2006 it was supposed to be covered by powdery gypsum with patches of halite, as explained in Section II and detailed in Table I. In any case, the agreement obtained for the TES retrievals over Lake Lucero at day and night was good, with the difference being less than ± 0.007 in all spectral bands. This is an encouraging result since ASTER/TES underestimates the emissivity of water by up to 3% in band 12 with mean differences of 2% for all bands and standard deviations of almost $\pm 1\%$ for bands 10–12 [10]. No laboratory spectrum was available for comparison with the April 2006 emissivities.

B. Emissivity Temporal Variation

Given the high-precipitation events that occurred during 2006 (see Fig. 3), the temporal variation of emissivities was studied from each target. Furthermore, ASTER emissivities were compared with the laboratory spectrum of water and gypsum and the basalt spectrum from [29] (see Table II) for the lava flow.

The precipitation data gave us an indication about the soil moisture conditions of the area during 2006. However, since the precipitation records are monthly values, it was not possible to know if the rain events occurred before or after the acquisition of the ASTER scenes. Furthermore, it is known that the sand in the upper dunes is easily air-blown and dried, while the gypsum in the lower interdune area has a compact wet texture and a

TABLE III
DAY/NIGHT ASTER EMISSIVITY DIFFERENCE ($\varepsilon_{\mathrm{ASTn}} - \varepsilon_{\mathrm{ASTd}}$) AT 180-m SPATIAL RESOLUTION, AND THEIR COMPARISON WITH THE CORRESPONDING LABORATORY SPECTRUM (i.e., GYPSUM OR WATER) FOR THE DIFFERENT SITES AND SPECTRAL BANDS. $|\Delta\varepsilon|_{\mathrm{av}}$ IS THE AVERAGE OF ABSOLUTE DIFFERENCES. EMISSIVITY DIFFERENCES GREATER THAN $\pm$ 0.016 ARE SHOWN FOR CLARITY

		$\varepsilon_{\mathrm{ASTn}} - \varepsilon_{\mathrm{ASTd}}$			$\varepsilon_{\mathrm{lab}} - \varepsilon_{\mathrm{ASTd}}$			$\varepsilon_{\mathrm{lab}} - \varepsilon_{\mathrm{ASTn}}$		
Sites	ASTER band	7 – 8 Apr '06	17 – 18 Nov '06	26 – 27 Apr '07	7 – 8 Apr '06	17 – 18 Nov '06	26 – 27 Apr '07	7 – 8 Apr '06	17 – 18 Nov '06	26 – 27 Apr '07
Dune-1	10	-0.001	0.003	0.000	**0.027**	**0.032**	**0.025**	**0.027**	**0.029**	**0.025**
	11	0.007	**0.049**	0.006	-0.013	-0.001	-0.015	**-0.020**	**-0.050**	**-0.021**
	12	0.003	0.010	0.012	-0.001	0.002	0.005	-0.004	-0.008	-0.007
	13	-0.003	-0.008	0.000	0.007	0.007	0.007	0.009	0.014	0.008
	14	-0.002	-0.008	0.000	0.007	0.005	0.008	0.009	0.013	0.009
Dune-2	10	-0.002	-0.001	-0.006	**0.016**	**0.021**	0.010	**0.018**	**0.022**	**0.015**
	11	0.000	0.010	-0.013	-0.001	0.006	-0.010	0.000	-0.003	0.003
	12	-0.001	0.000	0.007	0.001	0.004	0.010	0.002	0.005	0.003
	13	-0.002	-0.003	0.002	0.005	0.006	0.007	0.007	0.009	0.005
	14	0.000	-0.002	0.003	0.005	0.004	0.008	0.005	0.006	0.005
Lake Lucero	10	-0.001	0.000	0.001		*0.003*	*0.000*		*0.003*	*-0.001*
	11	-0.005	-0.005	-0.007		*0.001*	*-0.003*		*0.006*	*0.004*
	12	-0.002	0.001	0.004		*0.004*	*0.007*		*0.004*	*0.003*
	13	0.000	0.002	0.001		*-0.002*	*-0.001*		*-0.004*	*-0.001*
	14	0.000	0.002	-0.002		*-0.002*	*-0.002*		*-0.004*	*0.000*
Alkali Flat	10	0.003	0.002	-0.002						
	11	-0.012	**-0.032**	**-0.041**						
	12	-0.005	-0.012	-0.011						
	13	-0.002	0.002	0.001						
	14	0.000	0.003	0.001						
Dune-1	$\lvert\Delta\varepsilon\rvert_{\mathrm{av}}$	0.003	0.015	0.004	0.011	0.009	0.012	0.014	**0.02**	0.014
Dune-2		0.0010	0.003	0.006	0.006	0.008	0.009	0.006	0.009	0.006
Lake Lucero		0.0016	0.002	0.003	-	0.002	0.003	-	0.004	0.002
Alkali Flat		0.005	0.010	0.011	-	-	-	-	-	-

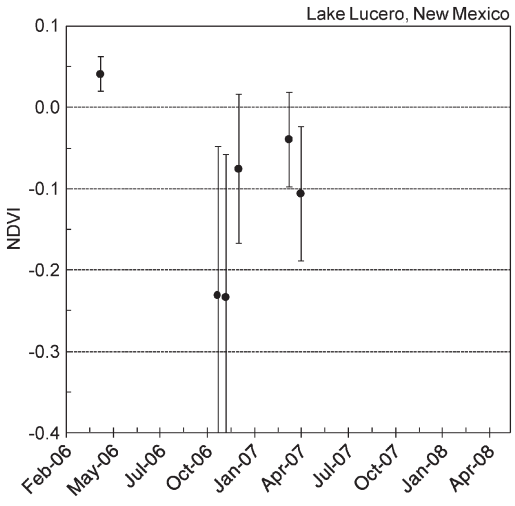

Fig. 6. Temporal variations in NDVI over Lake Lucero target for 2006–2007, derived from AST_07 standard product, degraded at 180-m spatial resolution. ASTER errorbars show spatial variation and correspond to the standard deviation of emissivities from that area.

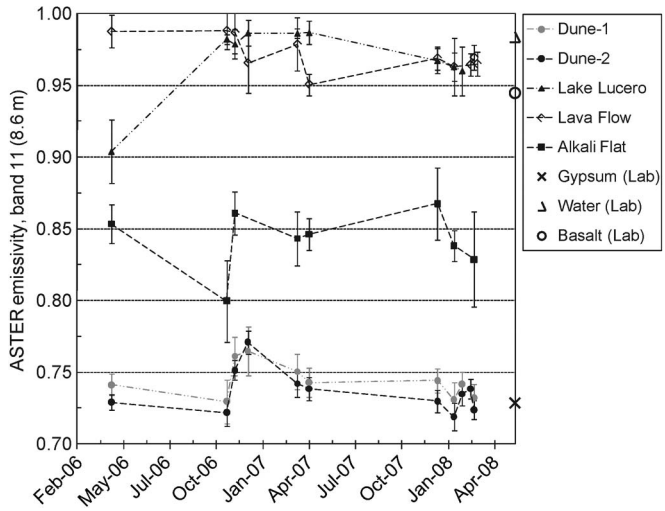

Fig. 7. Temporal variations of average 8.6-μm (ASTER band 11) emissivities retrieved from daytime ASTER acquisitions along years 2006–2008 from each studied target, compared with laboratory spectra of gypsum, water, and basalt.

slightly brown tint, showing more of a soil moisture effect on emissivity.

As an example of the emissivity temporal variation, Fig. 7 plots the average ASTER 8.6-μm emissivities retrieved during the years 2006–2008 from each studied target. This band was selected because it usually has the highest emissivity variation. This is observed qualitatively in Fig. 8, which presents the spectral shape retrieved from each ASTER scene and quantitatively studied in Table IV. At the same time, no significant ASTER emissivity change was observed over White Sands area from 2001 to 2003 by [30], an outcome consistent with a bare, dry gypsum surface and the lack of rains in that period.

Considering the soil moisture effect on TIR emissivities [31], low emissivity values were expected for the gypsum dunes (i.e., targets Dune-1 and Dune-2) during the dry period at the beginning of 2006 (i.e., from January to May, both included). Higher values were expected for the rainy period (i.e., from

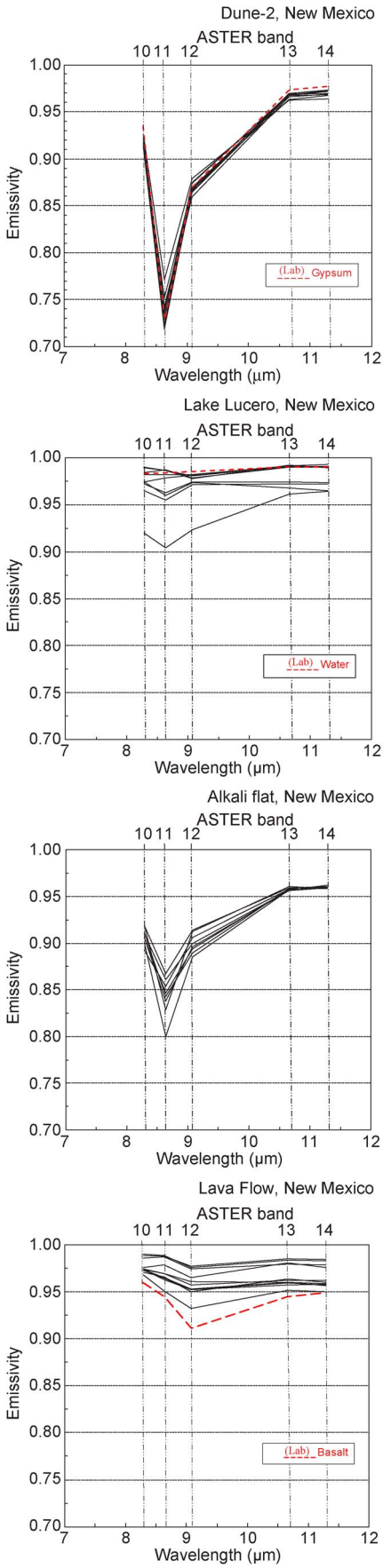

Fig. 8. Average spectral shape retrieved from each clear-sky ASTER scene acquired over the (black solid) studied targets in different dates, together with the (red dashed) laboratory spectra of water, gypsum, and basalt.

August to October, both included). However, unfortunately, no ASTER emissivity data were available during the rainy period, probably due to the presence of clouds. However, as summarized in Table IV, an emissivity increase up to 0.04 was observed at 8.6 μm (band 11) for the gypsum dunes between November and December 2006, months during which the precipitation totals were 0.05 and 0.71 cm, respectively. Hence, we consider that the increase of emissivities could be explained by previous rainfalls (even small) and related increase of soil moisture. Furthermore, from December 2006 to April 2007, an emissivity decrease up to 0.015 was observed for band 11 (8.3 μm), probably due to a decrease on soil water content because of higher temperatures and lower precipitation rates, particularly for bare surfaces as these are being studied. As observed before, when comparing the corresponding spectral shape of the observed emissivities with the laboratory spectra (Fig. 8), the agreement is quite good (i.e., average spectral agreement within ± 0.02).

For the Alkali Flat site, a similar increase was observed up to 0.06 at 8.6 μm (band 11) from November to December 2006 (see Table IV and Fig. 7). Furthermore, there was an emissivity variation during the years 2007 and 2008 of up to 0.03 for ASTER bands 10 (8.3 μm) and 12 (9.1 μm). However, as the area is not very homogeneous in emissivity (see error bars in Fig. 7, which correspond to standard deviation of emissivities from that area), the emissivity variability is not well defined, except for 10.7 μm (band 13) and 11.3 μm (band 14) where they remain almost constant along the time period.

The lava flow site is a rocky area with sparse vegetation. Hence, an increase of emissivities due to soil moisture is not observed here. On the contrary, an emissivity decrease of 0.02 is observed from November to December 2006 for all bands, being up to 0.03 at 9.1 μm (Table IV). After January 2007, a new decrease of emissivities is observed, probably due to the presence of senescent vegetation around the area. As plotted in Fig. 8, the spectral shape remains similar to that for basalt, as measured by [29], but not the amplitude, since it is not a barren area but a sparsely vegetated one, and emissivities are therefore higher.

As mentioned above, the cover type of Lake Lucero changed from powdery gypsum with patches of halite to water. It explains the temporal variation of emissivities observed for this site. The spectral shapes retrieved for this site agree with the emissivity of water (Fig. 8) when the lake was flooded and retains the low emissivity value of gypsum at 8.6 μm before the rain.

V. Summary and Conclusion

In this paper, the ASTER/TES emissivity product at 180-m spatial resolution was analyzed over an arid area in southern New Mexico during the period 2006–2008. The area provides an excellent test case for thermal remote sensing since it encompasses a broad range of emissivities from the high spectral contrast of gypsum desert areas of White Sands, the gray body behavior of water, or the high emissivity values over the lava flow. In addition, the effect of soil moisture on emissivity can be also studied, since heavy rainfall events in August 2006 contribute to flooded portions of the area.

TABLE IV
ASTER EMISSIVITY DIFFERENCE ($\Delta\varepsilon = \varepsilon_{\text{Dec'06}} - \varepsilon_{\text{Nov'06}}$) OBSERVED BETWEEN DAYTIME ACQUISITIONS FROM 18th NOVEMBER TO DECEMBER 29, 2006 AT THE DIFFERENT SITES

Sites	$\Delta\varepsilon = \varepsilon_{\text{Dec'06}} - \varepsilon_{\text{Nov'06}}$				
	ASTER b10 (8.3 μm)	ASTER b11 (8.6 μm)	ASTER b12 (9.1 μm)	ASTER b13 (10.7 μm)	ASTER b14 (11.3 μm)
Dune-1	0.016	0.04	0.010	-0.003	-0.006
Dune-2	0.013	0.05	0.014	-0.005	-0.009
Lake Lucero	0.007	0.004	-0.004	0.001	-0.003
Alkali Flat *	0.008	0.06	0.015	-0.001	-0.002
Lava Flow	-0.019	-0.02	-0.03	-0.02	-0.02

* No acquisition was taken over the Alkali Flat on 29th December, 2006; the acquisition on 4th December, 2006 was used instead.

Results of this study stress the need for further research on the operational ASTER/TES algorithm used to retrieve TIR emissivities for gray bodies, because the accurate determination of emissivity is important for accurate temperature retrievals and for the calculation of the longwave radiation balance. Furthermore, unexpected emissivity values larger than unity were retrieved by ASTER/TES at 8.3, 8.6, and 9.1 μm over the lava flow of the "Valley of Fires" in central New Mexico.

The main conclusions are that, generally, ASTER/TES works reasonably well, with a quantitative agreement (± 0.01–± 0.02) with laboratory measurements for emissivity, a repetivity better than ± 0.013, as shown by the day/night agreement, and the possibility of emissivity mapping on a regional scale. ASTER/TES works better for targets with large spectral contrasts, although quite good agreements were retrieved in this work for water targets (i.e., within ± 0.007).

ACKNOWLEDGMENT

The authors would like to thank the U.S. Geological Survey Earth Resources Observation and Science Data Center for supplying the ASTER data and the Jet Propulsion Laboratory (Pasadena, CA) for providing the laboratory emissivity spectra. Two anonymous referees have brought valuable comments and suggestions, which helped to improve this paper. The research described in this paper was carried out at the University of Valencia, Spain, under the support from the Spanish Ministry of Science and Innovation.

REFERENCES

[1] J. M. Norman and F. Becker, "Terminology in thermal infrared remote-sensing of natural surfaces," *Agr. Forest Meteorol.*, vol. 77, no. 3/4, pp. 153–166, Dec. 1995.

[2] M. Mira, E. Valor, R. Boluda, V. Caselles, and C. Coll, "Influence of soil water content on the thermal infrared emissivity of bare soils: Implication for land surface temperature determination," *J. Geophys. Res.*, vol. 112, no. F4, p. F04 003, 2007, DOI:10.1029/2007JF000749.

[3] Y. Yamaguchi, H. Fujisada, M. Kudoh, T. Kawakami, H. Tsu, A. B. Kahle, and M. Pniel, "ASTER instrument characterization and operation scenario," *Adv. Space Res.*, vol. 23, no. 8, pp. 1415–1424, 1999.

[4] Z. Wan, "New refinements and validation of the MODIS Land-Surface Temperature/Emissivity products," *Remote Sens. Environ.*, vol. 112, no. 1, pp. 59–74, Jan. 2008.

[5] J. Susskind, C. D. Barnet, and J. M. Blaisdell, "Retrieval of atmospheric and surface parameters from AIRS/AMSU/HSB data in the presence of clouds," *IEEE Trans. Geosci. Remote Sens.*, vol. 41, no. 2, pp. 390–409, Feb. 2003.

[6] L. C. Rowan, J. C. Mars, and C. J. Simpson, "Lithologic mapping of the Mordor, NT, Australia ultramafic complex by using the Advanced Spaceborne Thermal Emission and Reflection Radiometer (ASTER)," *Remote Sens. Environ.*, vol. 99, no. 1/2, pp. 105–126, Nov. 2005.

[7] R. G. Vaughan, S. J. Hook, W. M. Calvin, and J. V. Taranik, "Surface mineral mapping at Steamboat Springs, Nevada, USA, with multiwavelength thermal infrared images," *Remote Sens. Environ.*, vol. 99, no. 1/2, pp. 140–158, Nov. 2005.

[8] I. F. Trigo, L. F. Peres, C. C. DaCamara, and S. C. Freitas, "Thermal land surface emissivity retrieved from SEVIRI/Meteosat," *IEEE Trans. Geosci. Remote Sens.*, vol. 46, no. 2, pp. 307–315, Feb. 2008.

[9] K. Ogawa, T. Schmugge, and S. Rokugawa, "Estimating broadband emissivity of arid regions and its seasonal variations using thermal infrared remote sensing," *IEEE Trans. Geosci. Remote Sens.*, vol. 46, no. 2, pp. 334–343, Feb. 2008.

[10] G. C. Hulley and S. J. Hook, "The North American ASTER Land Surface Emissivity Database (NAALSED) version 2.0," *Remote Sens. Environ.*, vol. 113, no. 9, pp. 1967–1975, Sep. 2009.

[11] G. C. Hulley, S. J. Hook, and A. M. Baldridge, "Validation of the North American ASTER Land Surface Emissivity Database (NAALSED) version 2.0 pseudo-invariant sand dune sites," *Remote Sens. Environ.*, vol. 113, no. 10, pp. 2224–2233, Oct. 2009.

[12] R. P. Langford, "The holocene history of the White Sands dune field and influences on eolian deflation and playa lakes," *Quaternary Int.*, vol. 104, no. 1, pp. 31–39, 2003.

[13] R. J. Allmendinger, "Preliminary evaluation of the role of the hydrologic cycle in the development of the white sands, White Sands National Monument, New Mexico," in *Proc. Abstr. Programs Geological Soc. Amer.*, 1971, vol. 3, pp. 231–232.

[14] S. G. Fryberger, Geological Overview of White Sands National Monument, 2002. [Online]. Available: http://www.nps.gov/whsa/Geology

[15] H. Fujisada and A. Ono, "Anticipated performance of ASTER instrument in EM design phase," *Proc. SPIE*, vol. 1939, pp. 187–197, 1993.

[16] A. Gillespie, S. Rokugawa, T. Matsunaga, J. S. Cothern, S. Hook, and A. B. Kahle, "A temperature and emissivity separation algorithm for Advanced Spaceborne Thermal Emission and Reflection Radiometer (ASTER) images," *IEEE Trans. Geosci. Remote Sens.*, vol. 36, no. 4, pp. 1113–1126, Jul. 1998.

[17] V. J. Realmuto, "Separating the effects of temperature and emissivity: Emissivity spectrum normalization," in *Proc. 2nd TIMS Workshop*, Pasadena, CA, 1990, pp. 23–27.

[18] C. Coll, V. Caselles, E. Valor, R. Niclòs, J. M. Sánchez, J. M. Galve, and M. Mira, "Temperature and emissivity separation from ASTER data for low spectral contrast surfaces," *Remote Sens. Environ.*, vol. 110, no. 2, pp. 162–175, Sep. 2007.

[19] E. Valor and V. Caselles, "Mapping land surface emissivity from NDVI: Application to European, African, and South American areas," *Remote Sens. Environ.*, vol. 57, no. 3, pp. 167–184, Sep. 1996.

[20] W. T. Gustafson, A. R. Gillespie, and G. J. Yamada, "Revisions to the ASTER temperature/emissivity separation algorithm," in *Proc. 2nd Int. Symp. Recent Adv. Quantitative Remote Sens.*, Valencia, Spain, 2006, pp. 770–775.

[21] J. Labed and M. P. Stoll, "Angular variation of land surface spectral emissivity in the thermal infrared: Laboratory investigations on bare soils," *Int. J. Remote Sens.*, vol. 12, no. 11, pp. 2299–2310, Nov. 1991.

[22] J.-P. Lagouarde, Y.-H. Kerr, and Y. Brunet, "An experimental study of angular effects on surface temperature for various plant canopies and bare soils," *Agr. Forest Meteorol.*, vol. 77, no. 3/4, pp. 167–190, Dec. 1995.

[23] J. A. Sobrino and J. Cuenca, "Angular variation of thermal infrared emissivity for some natural surfaces from experimental measurements," *Appl. Opt.*, vol. 38, no. 18, pp. 3931–3936, Jun. 1999.

[24] J. Cuenca and J. A. Sobrino, "Experimental measurements for studying angular and spectral variation of thermal infrared emissivity," *Appl. Opt.*, vol. 43, no. 23, pp. 4598–4602, Aug. 2004.

[25] V. Garcıacute;a, M. Mira, E. Valor, V. Caselles, C. Coll, and J. M. Galve, "Angular dependence of the emissivity of bare soils in the thermal infrared," in *Proc. IEEE Int. Geosci. Remote Sens. Symp.*, Cape Town, South Africa, 2009, pp. III-133–III-136.
[26] A. M. Baldridge, S. J. Hook, C. I. Grove, and G. Rivera, "The ASTER spectral library version 2.0," *Remote Sens. Environ.*, vol. 113, no. 4, pp. 711–715, Apr. 2009.
[27] T. J. Schmugge, A. N. French, F. Jacob, K. Ogawa, J. C. Ritchie, M. J. Chopping, and A. Rango, "ASTER thermal infrared observations over New Mexico," in *Proc. SPIE—Remote Sensing for Agriculture, Ecosystems, and Hydrology IV*. M. Owe, G. D'Urso, and L Toulios, Eds., 2002, vol. 4879, pp. 166–173.
[28] J. W. Rouse, R. H. Haas, J. A. Schell, and D. W. Deering, "Monitoring vegetation systems in the great plains with ERTS," in *Proc. 3rd ERTS Symp.*, 1973, vol. 1, pp. 309–317.
[29] G. C. Hulley and S. J. Hook, "The ASTER Land Surface Emissivity Database (ALSED) of the USA—An update," in *Proc. ASTER Sci. Team Meeting*, Tokyo, Japan, Jun. 9–13, 2008.
[30] A. N. French, T. J. Schmugge, J. C. Ritchie, A. Hsu, F. Jacob, and K. Ogawa, "Detecting land cover change at the Jornada Experimental Range, New Mexico with ASTER emissivities," *Remote Sens. Environ.*, vol. 112, no. 4, pp. 1730–1748, Apr. 2008.
[31] M. Mira, E. Valor, V. Caselles, E. Rubio, C. Coll, J. M. Galve, R. Niclòs, J. M. Sánchez, and R. Boluda, "Soil moisture effect on thermal infrared (8–13 μm) emissivity," *IEEE Trans. Geosci. Remote Sens.*, vol. 48, no. 5, pp. 2251–2260, May 2010.

Maria Mira was born in Ontinyent, Spain, in 1982. She received the B.Sc. (first-class honors), M.Sc., and Ph.D. degrees in physics from the University of Valencia, Burjassot, Spain, in 2005, 2007, and 2010, respectively.

From December 2007 to March 2008, she was a Visiting Student with New Mexico State University, Las Cruces, and from September 2009 to December 2009, with National Institute for Agricultural Research, Bordeaux, France. She is currently with the Department of Earth Physics and Thermodynamics, Faculty of Physics, University of Valencia. Her research interest focuses on the physical processes of thermal-infrared remote sensing, including the retrieval of surface emissivity from thermal infrared remote sensed data supplied by the Moderate Resolution Imaging Spectroradiometer and the Advanced Spaceborne Thermal Emission and Reflection Radiometer sensors, as well as by field radiometers.

Thomas J. Schmugge (M'83–SM'91–F'01) received the B.S. degree in physics from the Illinois Institute of Technology, Chicago, in 1959 and the Ph.D. degree in physics from the University of California, Berkeley, in 1965.

From 1964 to 1970, he was an Assistant Professor of physics with Trinity College, Hartford, CT. For 15 years (1970–1986), he was with the Hydrological Sciences Branch, NASA Goddard Space Flight Center, Greenbelt, MD. In January 2004, he retired from the Hydrology and Remote Sensing Laboratory, Agricultural Research Service, U.S. Department of Agriculture, Beltsville, MD, where he worked on the application of remote sensing techniques to the study of land surface hydrologic processes. From 2005 to 2008, he was the Gerald Thomas Professor of water resources with New Mexico State University, Las Cruces. Currently, he is with the Physical Science Laboratory, New Mexico State University. He is an Adjunct Member of the Joint U.S./Japan Advanced Spaceborne Thermal Emission and Reflection Radiometer Science Team. He has published more than 250 papers on the application of remote sensing to hydrologic problems, more than half of which appeared in peer-reviewed journals. His research interests include the use of microwave and thermal infrared remote sensing techniques to observe such parameters as surface temperature and emissivity, soil moisture, and evapotranspiration.

Dr. Schmugge is a Fellow of the American Geophysical Union (AGU). He received the Robert E. Horton Medal in Hydrology from the AGU in 2006. He is an Associate Editor for the IEEE TRANSACTIONS ON GEOSCIENCE AND REMOTE SENSING.

Enric Valor received the B.Sc., M.Sc., and Ph.D. degrees in physics from the University of Valencia, Burjassot, Spain, in 1992, 1994, and 1997, respectively.

He is currently an Associate Professor of earth physics with the Department of Earth Physics and Thermodynamics, Faculty of Physics, University of Valencia. He has published 35 papers in international journals and 45 conference papers. His research interest focuses on the physical processes of thermal-infrared remote sensing, emissivity measurement and characterization, atmospheric and emissivity corrections, and temperature-emissivity separation algorithms.

Vicente Caselles received the B.Sc., M.Sc., and Ph.D. degrees in physics from the University of Valencia, Burjassot, Spain.

Currently, he is a Professor in applied physics and Head of the Thermal Remote Sensing Group with the Department of Earth Physics and Thermodynamics, University of Valencia, Burjassot, Spain. He has an expertise of 32 years in the physical processes involved in both temperature measurement and evapotranspiration using remote sensing techniques which has been documented through ten books, 20 doctoral theses, 100 papers in international journals, 60 conference papers, and 30 reports. He was collaborating with the European Space Agency as a member of the Advisory Group for the Land-Surface Processes and Interactions Mission. He was the Chairman of the Spanish Remote Sensing Society and, at present, he is the Manager of Human Resources and Researchers Mobility General Direction at the Spanish Ministry of Science and Innovation.

Dr. Caselles was the recipient of the Norbert Gerbier–MUMM International Award in 2010 conferred upon by the Executive Council of the World Meteorological Organization.

César Coll received the B.Sc., M.Sc., and Ph.D. degrees in physics from the University of Valencia, Burjassot, Spain, in 1989, 1992, and 1994, respectively.

He is currently an Associate Professor of earth physics with the Department of Earth Physics and Thermodynamics, Faculty of Physics, University of Valencia. He has published 40 papers in international journals and 50 conference papers. His research interest focuses on the physical processes of thermal-infrared (TIR) remote sensing, atmospheric and emissivity corrections, temperature-emissivity separation, and ground validation of Advanced Along Track Scanning Radiometer, Moderate Resolution Imaging Spectroradiometer, and Advance Spaceborne Thermal Emission and Reflection Radiometer TIR products.